Journal of Minerals and Materials Characterization and Engineering, 2026, 14(1), 15-25
https://www.scirp.org/journal/jmmce
ISSN Online: 2327-4085
ISSN Print: 2327-4077

Anisotropy on Mechanical Properties of CMSX-6 Ni-Base Superalloy Single Crystal Using Profilometer Indentation Plastometer (PIP) and Small Punch Test (SPT)

Daniel Moreno[1*], Amit Yair[2], Libi Shechner[1], Yohanan Nahmana[1], Ariel Yehuda Cohen[1], Moshe Shapira[1]

[1]Bet Shemesh Engines Ltd., FAA & EASA, Bet Shemesh, Israel
[2]Azrieli College, Jerusalem, Israel
Email: *danielm@bsel.co.il

How to cite this paper: Moreno, D., Yair, A., Shechner, L., Nahmana, Y., Cohen, A.Y. and Shapira, M. (2026) Anisotropy on Mechanical Properties of CMSX-6 Ni-Base Superalloy Single Crystal Using Profilometer Indentation Plastometer (PIP) and Small Punch Test (SPT). *Journal of Minerals and Materials Characterization and Engineering*, **14**, 15-25.
https://doi.org/10.4236/jmmce.2026.141002

Received: November 9, 2025
Accepted: January 18, 2026
Published: January 21, 2026

Abstract

Validating alternative techniques for accurately determining true mechanical properties—particularly yield stress, which cannot be reliably derived from hardness testing—remains a significant challenge. In this work, we investigate the anisotropy of the mechanical properties of the CMSX-6 Ni-base superalloy single crystal using both the Profilometry-based Indentation Plastometry (PIP) and the Small Punch Test (SPT). The obtained results are compared with each other and with values reported in the literature. This study examines the complex interpretation of mechanical property data obtained from three experimental approaches and explores how these results can be correlated. One of the main challenges addressed is the characterization of a highly anisotropic material—a nickel-based single crystal—in its three principal crystallographic orientations, <001>, <101>, and <111>, to assess the accuracy of the employed techniques. The results demonstrate that the combined use of the PIP and SPT methods provides consistent and reliable measurements, with an estimated deviation of less than 12% in the yield stress obtained.

Keywords

Mechanical Properties, Anisotropy, Ni-Base Single Crystal, Small Punch Test (SPT), Profilometry-Based Indentation Plastometer (PIP)

1. Introduction

Over the past two decades, the need to simplify the testing of mechanical proper-

ties in metals has become increasingly important—particularly for acceptance processes, post-service life assessment, irradiated materials, and additively manufactured components. Validating alternative techniques to accurately determine true mechanical properties—especially yield stress, which cannot be reliably obtained from hardness testing—remains a significant challenge. The initial motivation for developing small specimen testing arose at the beginning of the 1980s in the nuclear industry, due to the limited number of irradiated standard specimens [1]. Small specimens could be extracted from the fragments of the already tested standard specimens in such a way that properties can be compared and evaluated. (SPT)/Ball Punch Test (BPT) [2] [3] or Disk Bend Test (DBT) [1], as well as Shear Punch Test [4]-[8] and others, are techniques developed to characterize the mechanical behavior of small or thin specimens. The SPT concept involves two dies clamping a thin sample foil, typically around half a millimeter thick, while a hard ball presses against it, deforming it into a spherical shape until failure occurs. The displacement of the hard ball during thin foil deformation under increasing load is plotted concurrently, up to the point at which the load drops because of foil sample failure. Different empirical correlation functions were used to extract the main mechanical values, such as yield and ultimate stress, from the SPT plot described above. It is possible to consider that the best estimation for the yield and ultimate stress can be obtained by [9]:

$$\sigma_{\mathrm{y}} = \alpha_1 \cdot \frac{\mathrm{F_e}}{(\mathrm{t})^2} + \alpha_2 \tag{1}$$

$$\sigma_{\mathrm{UTS}} = \beta_1 \cdot \frac{\mathrm{F_{max}}}{(\mathrm{t} \cdot \delta_m)} + \beta_2 \tag{2}$$

where σ_{y} is the yield stress, $\mathrm{F_e}$ is the applied load in the bending assumed as a metal yield, σ_{UTS} is the ultimate tensile stress, and $\mathrm{F_{max}}$ is the maximum applied load in the plot. Here, δ_m is the maximal punch deflection at maximal load and t is the thickness of the sample. The coefficients α_1 and α_2 provide a good approximation for the yield stress and β_1 and β_2 are the ultimate tensile stress of many of the tested materials.

Finite element simulations of the SPT were used to understand the sensitivity of the specimen thickness variations [2]. A review and assessment of the ongoing development of the Small Punch Test (SPT) highlights its strengths and existing knowledge gaps and emphasizes the need for further optimization and standardization to enhance its effectiveness in characterizing the mechanical properties of materials [10].

On the other hand, a highly advanced technique known as Profilometry-based Indentation Plastometer (PIP) utilizes the pile-up deformation produced by a ball indentation to extract tensile stress-strain characteristics. The PIP method involves measuring the full indentation profile and applying automated, iterative Finite Element Modeling (FEM) to simulate the indentation process, enabling the accurate determination of the complete true stress-strain curve. Southern *et al.* [11] examine the application of various approaches to different alloys, comparing the inferred

stress-strain characteristics with those obtained through tensile testing. The study offers insights into the contrasting levels of detail and reliability provided by each method. In their work, they conclude that the Ultimate Tensile Strength (UTS) is a nominal stress value meaningful only within the context of uniaxial tensile testing. While it may correlate with Brinell hardness in some cases, it provides no information about the onset of yielding or any characteristics of the true stress-strain curve. In mechanical engineering, one of the most critical material properties is the yield stress. This value is essential for predicting how components or structures will respond to loading conditions that may lead to inelastic (plastic) deformation. The proposed PIP technique leverages the complete indentation profile, which contains detailed quantitative information about work hardening behavior influenced by the yield stress. Using iterative FEM simulation, the yield stress and other stress-strain curve properties can be automatically extracted from this profile [11]. CORSICA, a software developed by Plastometrex© (Cambridge, England), is used to calculate stress-strain curves from indentation test data collected using the Indentation Plastometer©. It employs an accelerated inverse finite element method to rapidly and accurately extract material properties. The software outputs both true and nominal (engineering) stress-strain curves and infers key plasticity parameters, including yield stress, Ultimate Tensile Strength (UTS), uniform elongation strain, and strain hardening behavior, which is characterized using the Voce hardening law [12]. One disadvantage of the PIP is that the indentation occurs in a very small region of the sample, involving only a limited number of grains beneath the indenter. In some cases, the interface may lie within a single grain. When this happens, the anisotropy of the crystallographic structure can significantly affect the accuracy of the results. In contrast, anisotropy effects are not expected in the Small Punch Test (SPT), as a much larger number of grains are involved in the deformation process.

In the present work, we examine the anisotropy of the mechanical properties of the CMSX-6 Ni-base single-crystal superalloy using both the Profilometer Indentation Plastometer (PIP) and the Small Punch Test (SPT), and we compare the results obtained from these techniques. The main contribution of this study is the use of PIP-derived data to calibrate the empirical correlation used in SPT analysis by exploiting the intrinsic anisotropy of a single-crystal metal.

2. Experimental

A single-crystal Ni-based CMSX-6 superalloy rod was grown using an ALD directional solidification furnace along the <001> direction, with an orientation accuracy better than 10 degrees. The 12 mm rod was sectioned into flat samples with a thickness of 0.7 mm along the <001>, <011>, and <111> crystallographic directions, as shown in **Figure 1**. These samples were polished using 600-grit silicon carbide abrasive paper and prepared for Small Punch Testing (SPT). Additionally, three separate samples with a thickness greater than 3 mm were prepared for PIP. To ensure reliable results, at least three indentations were carried out and the values were averaged using the PIP technique. The SPT experiments were conducted

using a custom-designed puncher equipped with a 4.763 mm diameter chromium steel (AISI 52100) ball, as shown in **Figure 2**. The load was applied using a standard Instron testing machine operating in stroke-controlled mode. Load-displacement data were acquired automatically, and the resulting data were analyzed according to the methodology reported in ref. [2] [13]. The PIP test was conducted using a PLX-Benchtop device, a commercially available system that employs a Profilometry-based Indentation Plastometer (PIP), as shown in **Figure 3**, to generate the stress-strain behavior of the samples.

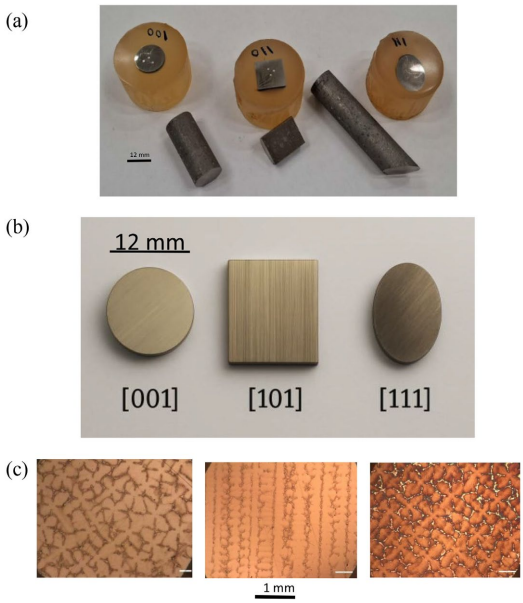

Figure 1. The cut CMSX-6 single crystal rod after cut at <001>, <011> and <111> crystallographic directions and cold mount of cut samples for the PIP test (a), slide examples for the STP (b), and metallographic microstructure of the sample at 3 crystallographic direction, respectively (c).

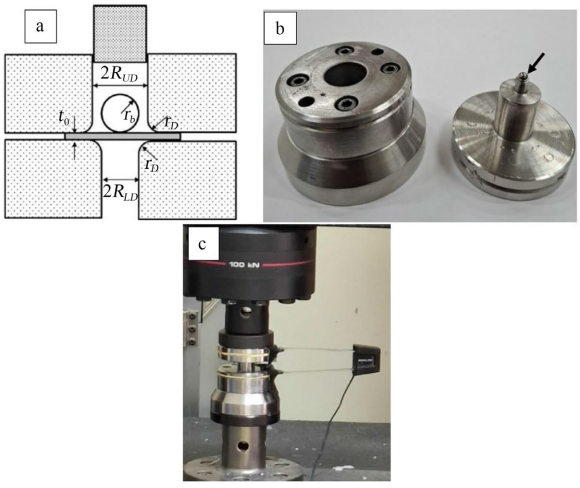

Figure 2. SPT device: (a) Schematic concept punch, (b) the punch used (the ball signed by an arrow), and (c) the measurement configuration under the load machine and the attached extensometer.

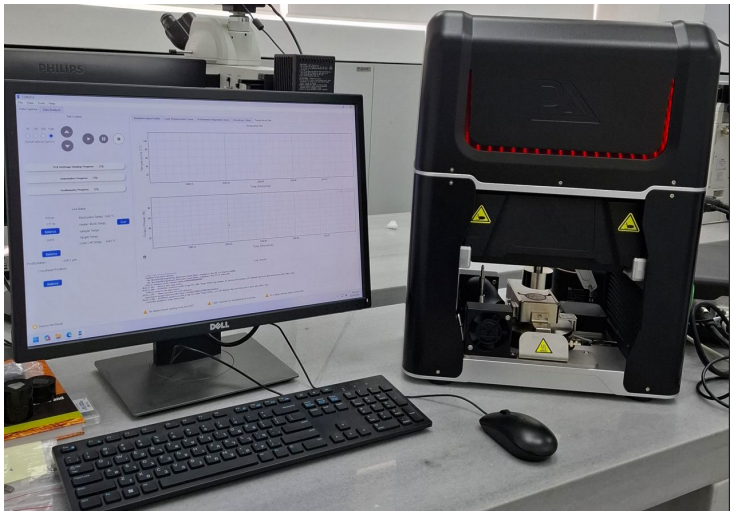

Figure 3. PLX-Benchtop device, a commercially available system that employs a Profilometry-based Indentation Plastometer (PIP) [11] [12].

3. Results

A representative displacement–load curve corresponding to the punch deflection obtained from the SPT is shown in **Figure 4**. The empirical procedure used to determine the yield load and maximum load from each plot follows the methodology described in [13]. Two sets of data were used for the empirical forced correlations to establish the α and β coefficients: one set derived from literature data, and another obtained using the PIP technique in this study. The coefficients determined in this work were obtained by correlating the calculated Fe/t^2 and $F_{max}/t \times \delta$ experimental values with the corresponding σ_{yield} and σ_{UTS} values, obtained either from the literature or from PIP experiments, respectively. This forced graphical correlation—from smaller to larger values—assumes the existence of a valid empirical relationship, although it is not necessarily a direct mathematical one. The slopes of the forced linear regressions, adapted to the reported values in [14]-[17] for the first dataset and to the PIP data for the second, are shown in **Figures 5-8**. The α and β coefficients were extracted by linear regression, respectively. Using these coefficients, the yield stress and ultimate tensile stress for each crystallographic direction were calculated according to Equations (1) and (2), and the results are summarized in **Table 1**. For comparison, the PIP results obtained from samples prepared from the same rod and crystallographic directions as those used in the SPT, along with equivalent values reported in [14] [15] [17], are also summarized in **Table 1**. Fractographic analysis of the punched samples in each crystallographic direction was carried out using Scanning Electron Microscopy (SEM), and the results are presented in **Figure 9**. The micrographs reveal the presence of multiple slip planes associated with the [111] <101> slip system, characteristic of the FCC phase of the Ni-base single crystal. This multi-slip deformation is particularly evident in the [111] sample, as shown in **Figure 9(c)**, and is also observed in the [101] sample, shown in **Figure 9(b)**.

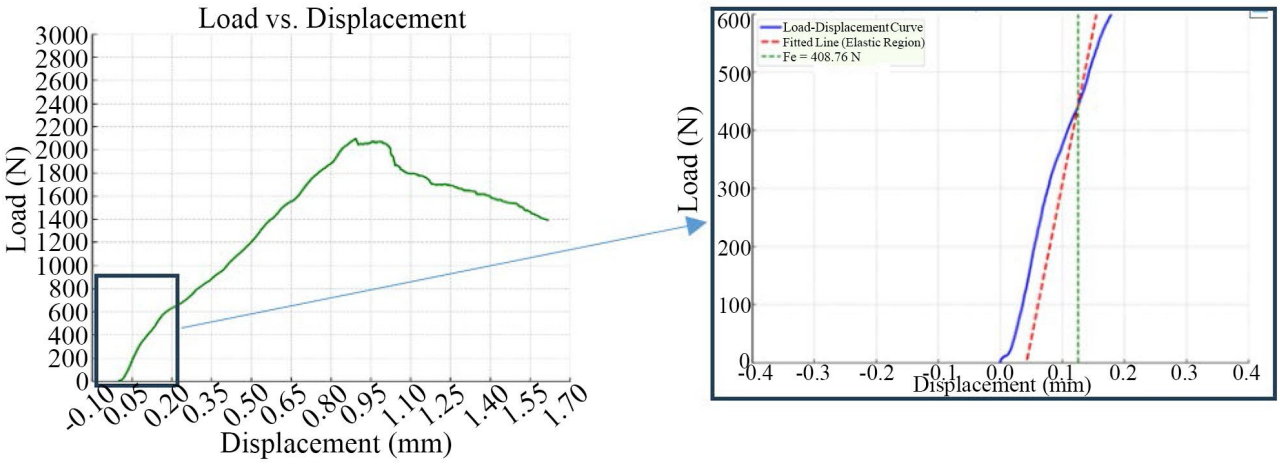

Figure 4. Left, displacement vs. load obtained the SPT technique and, right, the Fe load obtained by the t/10 shifted line parallel to the elastic range in displacement vs. load curve.

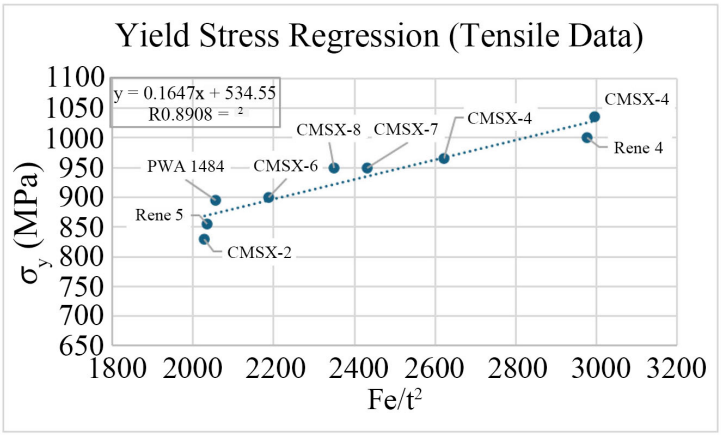

Alloy	Yield [MPa]	Orientation	Fe/t² [MPa]
CMSX-2	830	[101]	2027.484
Rene 5	855	[101]	2034.903
PWA 1484	895	[001]	2055.111
CMSX-6	900	[101]	2187.885
CMSX-8	950	[001]	2349.512
CMSX-7	950	[001]	2431.947
CMSX-4	966	[111]	2621.65
Rene 4	1000	[111]	2976.598
CMSX-4	1035	[111]	2995.169

Figure 5. The α coefficients were determined from the empirical slope of the linear regression of Fe/t², forced to be adapted to the σ_{yield} reported elsewhere [14]-[17]. Fe is the yield load from the SPT curve, and t is the sample thickness. The regression analysis yielded a value of $\alpha_1 = 0.1647$, $\alpha_2 = 537$.

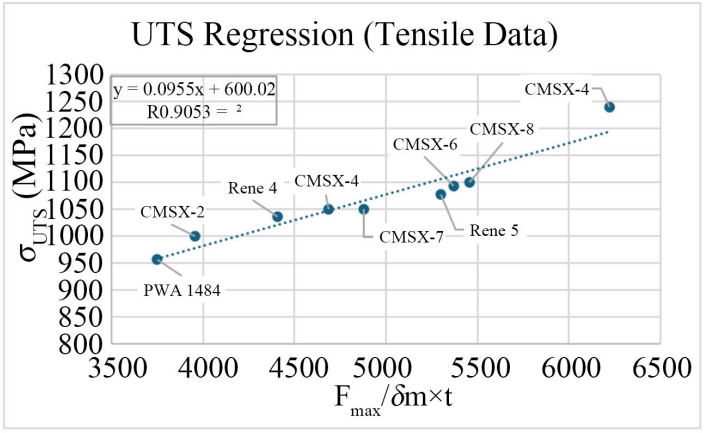

Alloy	UTS [MPa]	Orientation	$F_{max}/t\times\delta$
PWA 1484	957	[001]	3745.779
CMSX-2	1000	[101]	3953.633
Rene 4	1036	[111]	4407.113
CMSX-4	1050	[101]	4684.371
CMSX-7	1050	[001]	4876.997
Rene 5	1078	[001]	5301.252
CMSX-6	1092.5	[111]	5368.818
CMSX-8	1100	[101]	5454.997
CMSX-4	1240	[111]	6222.714

Figure 6. The β coefficients were determined from the empirical slope of the linear regression of Fe/t², forced to be adapted to the σ_{UTS} reported elsewhere [13]-[16]. Fe is the yield load from the SPT curve, and t is the sample thickness. The regression analysis yielded a value of $\beta_1 = 0.0955$, $\beta_2 = 600$.

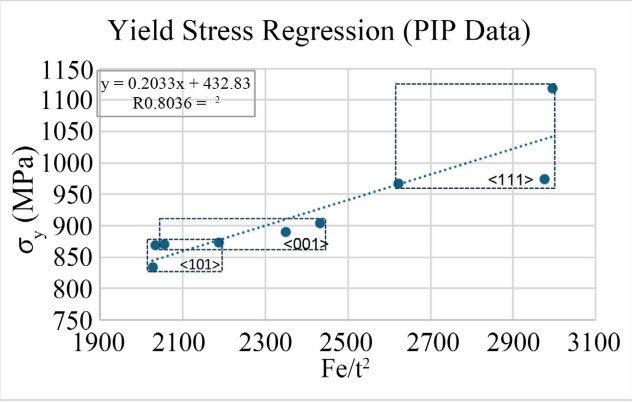

Orientation	PIP Yield [MPa]	Fe/t² [MPa]
[101]	834	2027.484
[101]	869	2034.903
[001]	871	2055.111
[101]	873	2187.885
[001]	891	2349.512
[001]	905	2431.947
[111]	967	2621.65
[111]	975	2976.598
[111]	1119	2995.169

Figure 7. The α coefficients were determined from the empirical slope of the linear regression of Fe/t², forced to be adapted to the σ_{yield} obtained by the PIP experiments in this work. Fe is the yield load from the SPT curve, and t is the sample thickness. The regression analysis yielded a value of $\alpha_1 = 0.2033$, $\alpha_2 = 433$ (The square boxes show the yield obtained by PIP for each direction).

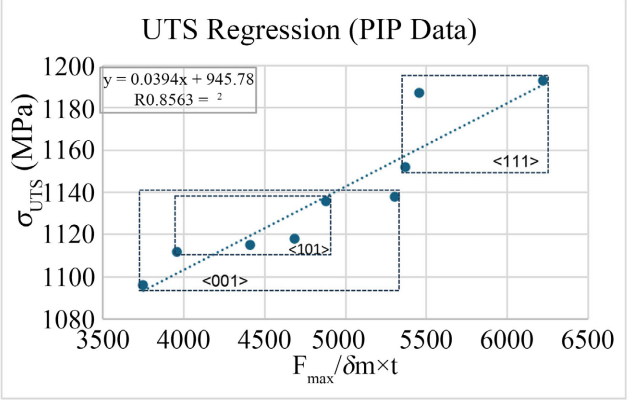

Orientation	PIP UTS [MPa]	$E_{max}/t\times\delta$
[001]	1096	3745.779
[101]	1112	3953.633
[101]	1115	4407.113
[001]	1118	4684.371
[101]	1136	4876.997
[001]	1138	5301.252
[111]	1152	5368.818
[111]	1187	5454.997
[111]	1193	6222.714

Figure 8. The β_1 coefficient was determined from the empirical slope of the linear regression of Fe/t², forced to be adapted to the σ_{UTS} obtained by the PIP experiments in this work. Fe is the yield load from the SPT curve, and t is the sample thickness. The regression analysis yielded a value of $\beta_1 = 0.0394$, $\beta_2 = 946$ (The square boxes show the UTS obtained by PIP for each direction).

Table 1. Summarized yield stresses and UTS for each crystallographic direction, obtained by SPT, PIP and standard tests.

Orientation	SPT α_1=0.1647, α_2 = 535 (R_2 = 0.8908) β_1 = 0.0955, β_2 = 600 (R_2 = 0.8563) [13]-[16]		SPT α_1 = 0.203, α_2 = 432 (R_2 = 0.8036) β_1 = 0.0394, β_2 = 946 (R_2 = 0.8563) based on PIP in this work		PIP		Standard Stress-Strain [13] [14]		Higher to Δ% Lower	Remarks
Properties	S_{yield} [MPa]	S_{UTS} [MPa]	S_{yield} [MPa]	S_{UTS} [MPa]	S_{yield} [MPa]	S_{UTS} [MPa]	S_{yield} [MPa]	S_{UTS} [MPa]	S_{UTS} [MPa]	
<001>	928 ± 22	1060 ± 43	917 ± 27*	1135 ± 18*	889**	1117**	847⁺ 835⁺⁺	905⁺ 1220⁺⁺	1135 ± 18*	3 - 5 tests* Average of 3 tests** CMSX6⁺ [13] N4⁺⁺ [14]
<011>	863 ± 14	1012 ± 46	839 ± 18*	1116 ± 19*	859**	1121**	840⁺⁺	**850⁺⁺**	1116 ± 19*	
<111>	1006 ± 20	1109 ± 50	1015 ± 24*	1155 ± 20*	1020**	1117**	1220⁺⁺	**1600⁺⁺**	1155 ± 20*	

The symbol * for the YIELD stresses and UTS stresses, said that the value was obtained by 3 up to 5 reported experiments presented with the standard deviation of them. The symbol ** as well, but the average was presented. Symbol + are singular reported values obtained from ref. [13] and symbol ++ from ref. [14]

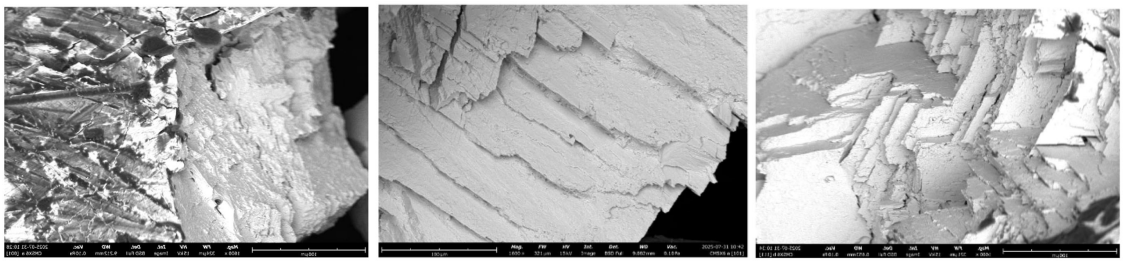

(a) (b) (c)

Figure 9. SEM images of cracks formed during SPT failure after application of the maximum load (Fmax) for samples oriented along (a) [001], (b) [101], and (c) [111], all shown at the same magnification. Pronounced slip planes are observed in the [101] and [111] orientations.

4. Discussion

The present work investigates the complex interpretation of mechanical property data obtained from three experimental modes and explores how these results can be correlated with one another. Standard alloy data sheets and previously published reports were used as primary references for establishing these correlations. In many cases—particularly when the material is unknown, it has undergone metallurgical changes, or has been subjected to long-term service—performing a standard tensile test becomes impossible due to the insufficient amount of material available to prepare a standard specimen. The newly developed Profilometry-based Indentation Plastometry (PIP) technique offers a valuable alternative in such situations, provided that the sample has a minimum thickness of 3 mm and that sufficient material is available. In many situations, this is not the case. Often, we only have a thin piece of metal (such as blades), which makes the use of the PIP technique impractical. In such cases, the STP technique can be applied instead. Although this method does not provide yield or Ultimate Tensile Strength (UTS) values, it can still produce results that are useful for comparison with similar specimens tested in the standard metallurgical condition. Despite the standard tensile test, both the PIP and SPT techniques have certain limitations related to factors such as the number of grains within the indented zone, material anisotropy, multiaxial stresses and strains, and geometric constraints like minimum sample thickness. The PIP test, which typically uses a 0.5 - 1 mm ball diameter, probes a very small region—sometimes encompassing only a single grain. In contrast, the SPT technique offers an advantage when characterizing thin foils, as the tested area includes a larger number of grains, providing more representative results. Nevertheless, in this work, we eliminate grain-boundary effects by using single-crystal samples of different orientations, allowing us to highlight the intrinsic anisotropy of the mechanical properties in each direction. Both techniques, PIP and SPT, are not included in the world standards and are not widely recommended for use when sufficient material is available to prepare standard samples and when there is enough time to fully characterize the metal. Instead, they are typically applied only when such options are not available. Another noteworthy application is in the characterization of anisotropy in additively manufactured metals [18]. One of

the main challenges of the present work is to characterize a highly anisotropic material—specifically, a nickel-based single crystal—in its three principal orientations <001>, <101> and <111>. The goal is to investigate how the mechanical properties of the same metal vary with orientation, to assess the sensitivity of the applied characterization techniques. In this case, the effect of grain boundaries is neglected; however, as expected, consistent variations in yield stress and Ultimate Tensile Strength (UTS) are observed depending on the crystallographic orientation. This sensitivity demonstrates that the applied techniques are suitable for characterizing additively manufactured materials using very small samples, provided that proper calibration is performed through a reliable correlation of results to obtain the α and β coefficients required for production quality control and repeatability. The results presented in Table 1 show fair agreement among the three techniques, even though the comparison was based on a forced correlation between the values obtained through empirical regression. In some cases, the ultimate stresses reported in other sources are excessively high and widely scattered, preventing an accurate calculation of the deviation. These variations in the reported values can be attributed to differences in the metallurgical condition of the samples, which limit direct comparison with the results obtained in this work. Nevertheless, from an engineering perspective, the most critical parameter is the yield stress as mentioned above. In this study, a deviation of approximately 10% was achieved using the PIP empirical correlation. The independent correlation presented in Table 1 between the results obtained using the PIP technique—performed on the same rod, material, and orientation as the SPT measurements—and those derived from data sheets and reports, provides strong confidence in the combined use of PIP and SPT methods. This combined approach has proven to be highly valuable from a technological standpoint, particularly in cases where PIP and SPT are the only feasible techniques for determining the yield stress when standard tensile testing cannot be performed.

5. Conclusions

In the present work, the SPT technique was used to estimate the yield stress and UTS of an anisotropic Ni-based single crystal in the three principal orientations <001>, <101>, and <111>, showing trends consistent with well-established results reported in the literature.

The SPT technique is not an independent technique and forced empirical regression with results obtained somewhere else is needed.

Empirical regression by using PIP results presents good agreement and α and β coefficients can be subtracted from the forced empirical correlation that can be used for future SPT measurements in similar materials.

Conflicts of Interest

The authors declare no conflicts of interest regarding the publication of this paper.

References

[1] Corwin, W.R. and Lucas, G.E. (1983) The Use of Small-Scale Specimens for Testing Irradiation Materials. A Symposium Sponsored by ASTM Committee E-10, ASTM Publication. https://compass.astm.org/document/?contentCode=ASTM%7CSTP888-EB%7Cen-US&proxycl=https%3A%2F%2Fsecure.astm.org&fromLogin=true

[2] Haroush, S., Priel, E., Moreno, D., Busiba, A., Silverman, I., Turgeman, A., *et al.* (2015) Evaluation of the Mechanical Properties of SS-316L Thin Foils by Small Punch Testing and Finite Element Analysis. *Materials & Design*, **83**, 75-84. https://doi.org/10.1016/j.matdes.2015.05.049

[3] Snir, Y., Moreno, D., Silverman, I., Samuha, S., Eisen, Y., Eliezer, D., *et al.* (2020) Mechanical Properties of Proton Bombarded SS316L Thin Foils Using the Small Punch Technique. *Journal of Nuclear Materials*, **540**, Article ID: 152340. https://doi.org/10.1016/j.jnucmat.2020.152340

[4] Guduru, R.K., Darling, K.A., Kishore, R., Scattergood, R.O., Koch, C.C. and Murty, K.L. (2005) Evaluation of Mechanical Properties Using Shear-Punch Testing. *Materials Science and Engineering*: *A*, **395**, 307-314. https://doi.org/10.1016/j.msea.2004.12.048

[5] Hamilton, M.L. and Toloczko, M.B. (2000) Effect of Low Temperature Irradiation on the Mechanical Properties of Ternary V-Cr-Ti Alloys as Determined by Tensile Tests and Shear Punch Tests. *Journal of Nuclear Materials*, **283**, 488-491. https://doi.org/10.1016/s0022-3115(00)00227-0

[6] Toloczko, M.B., Kurtz, R.J., Hasegawa, A. and Abe, K. (2002) Shear Punch Tests Performed Using a New Low Compliance Test Fixture. *Journal of Nuclear Materials*, **307**, 1619-1623. https://doi.org/10.1016/s0022-3115(02)01258-8

[7] Hankin, G.L., Toloczko, M.B., Hamilton, M.L., Garner, F.A. and Faulkner, R.G. (1998) Shear Punch Testing of 59ni Isotopically-Doped Model Austenitic Alloys after Irradiation in FFTF at Different HE/DPA Ratios. *Journal of Nuclear Materials*, **258**, 1657-1663. https://doi.org/10.1016/s0022-3115(98)00204-9

[8] Goyal, S., Karthik, V., Kasiviswanathan, K.V., Valsan, M., Rao, K.B.S. and Raj, B. (2010) Finite Element Analysis of Shear Punch Testing and Experimental Validation. *Materials & Design* (1980-2015), **31**, 2546-2552. https://doi.org/10.1016/j.matdes.2009.11.031

[9] García, T.E., Rodríguez, C., Belzunce, F.J. and Suárez, C. (2014) Estimation of the Mechanical Properties of Metallic Materials by Means of the Small Punch Test. *Journal of Alloys and Compounds*, **582**, 708-717. https://doi.org/10.1016/j.jallcom.2013.08.009

[10] Torres, J. and Gordon, A.P. (2021) Mechanics of the Small Punch Test: A Review and Qualification of Additive Manufacturing Materials. *Journal of Materials Science*, **56**, 10707-10744. https://doi.org/10.1007/s10853-021-05929-8

[11] Southern, T.J.F., Campbell, J.E., Fang, C., Nemcova, A., Bannister, A. and Clyne, T.W. (2023) Use of Hardness, PIP and Tensile Testing to Obtain Stress-Strain Relationships for Metals. *Mechanics of Materials*, **187**, Article ID: 104846. https://doi.org/10.1016/j.mechmat.2023.104846

[12] Plastometrex. https://www.plastometrex.com/corsica

[13] Lancaster, R.J., Jeffs, S.P., Haigh, B.J. and Barnard, N.C. (2022) Derivation of Material Properties Using Small Punch and Shear Punch Test Methods. *Materials & Design*, **215**, Article ID: 110473. https://doi.org/10.1016/j.matdes.2022.110473

[14] Zheng, S., Zhang, J., Liu, Y.F., Xu, J.W., Zhang, X.N. and Cui, L.L. (2024) Microstructure and Mechanical Properties of a First-Generation Single Crystal Superalloy CMSX-6. *Journal of Physics*: *Conference Series*, **2686**, Article ID: 012015. https://doi.org/10.1088/1742-6596/2686/1/012015

[15] Petrushin, N.V., Svetlov, I.L. and Khvatskiy, K.K. (2010) Anisotropy of Mechanical Proper-Ties of Single Crystal in Fourth Generation Ni-Based Superalloy. All-Russian Institute of Aviation Materials (VIAM). https://www.eucass.eu/component/docindexer/?task=download&id=4424

[16] High-Temperature High-Strength Ni-Base Alloys—A Practical Guide to the Use of Ni-Containing Alloys No. 393, Nickel Institute. https://www.nickelinstitute.org

[17] Neway Precision LTD. https://www.newayaerotech.com/services/single-crystal-casting

[18] Moreno, D., Nahmana, Y., Nafman, O., Kam, O., Wolfman, B., Cohen, A.Y., *et al.* (2022) Mechanical Properties, Metallurgical Characteristics and Anisotropy of Additive Manufacturing of 316l. *Journal of Minerals and Materials Characterization and Engineering*, **10**, 209-223. https://doi.org/10.4236/jmmce.2022.102017